

# Introduction to SNANA

II

*A common mistake that people make when trying  
to design something completely foolproof is to  
underestimate the ingenuity of complete fools*

Douglas Adams, *Mostly Harmless*

We have seen Chapter ?? that from 1993, thanks to the standardization of the SNe Ia by the study of their characteristics of stretching and color in particular, the cosmology based on the SNe Ia was able to prosper, giving an uncertainty on the modules of distances of approximately 15%; if that was enough to improve the precision of the time, dominated by the statistical uncertainties, the principal source of error on the measurements of cosmological parameters became since the systematic uncertainty.

To this end, the SuperNova ANALysis software package (SNANA, [Kessler et al. 2009b](#)) attempts to homogenize the different cosmological analyses through a reliable tool with reproducible procedures and scalable implementations. The versatility of this project makes it a widely used tool in cosmology (e.g., [Kessler et al. 2009a](#); [Conley et al. 2011](#); [Betoule et al. 2014](#); [Smith et al. 2020](#)) whether to study a specific survey or a combination of surveys. It is therefore natural that after studying the evolution of SNe Ia properties in correlation with their Chapter? **Chapter ?**, we have turned to this software to estimate the impact of this modeling on the determination of cosmological parameters.

We introduce the package in this chapter. We start with the background of its establishment Section [I.1](#), before detailing the three key steps of its operation: the simulation (Section [I.2](#)), the fitting of light curves (Section ?? ) and the correction of distance biases and the calculation of cosmological parameters (Section [I.3](#)).

## Contents

<b>I.1 Context.....</b>	<b>2</b>
<b>I.2 Simulation.....</b>	<b>2</b>
I.2.1 Preparing a simulation ... ..	2
I.2.2 Model generation ... ..	5
I.2.3 Instrumental response ... ..	7
I.2.4 Selection and adjustment... ..	7
I.2.5 Summary ... ..	8
<b>I.3 Bias correction and cosmology.....</b>	<b>8</b>
I.3.1 Presentation . . . . .	8
I.3.2 BBC1D11	
I.3.3 BBC5D11	
I.3.4 BBC7D14	

## I.1 Context

It is in the context of the diversity of cosmological analyses, particularly the diversity of light curve fitting software, that the SNANA package was born (Kessler et al. 2009b). Its objective is to provide the different groups with a public and reliable tool allowing reproducibility of the analyses. It is a package of software, including a light curve adjuster, a Monte Carlo simulator, and a cosmology adjuster, simulating data catalogs rather than survey images for greater efficiency. The software integrates existing models but also offers the possibility to adapt to new models, not limited to SNe Ia (there are for example Kilo Novae models) and admitting since then correlations between a SN and its environment, which have become as important as the goodness of fit as discussed in Chapter ?

Indeed, the past decade has seen many efforts directed toward implementing quality simulations to correct for redshift-dependent biases in the distance module caused by selection effects, and SNANA establishes a framework for simulating these effects for different surveys (Kessler et al. 2019). These effects can be of various origins: from the limiting magnitude of the instruments causing Malmquist bias, as presented in Chapter ? but also from the quality of the transient detection procedures, the choice of candidates for spectro-photometric monitoring or the criteria for selecting data considered as cosmologically valid (see Chapter ?? ). Figures 4 to 7 of Chapter ?? are indeed taken from simulations, and indicate a bias of up to 0.10 mag. Finally, the biases on the distance modulus also depend on the parent populations of the stretch and color of a SN Ia but also on the intrinsic variabilities of magnitude: it is this part specifically that is under study in our thesis.

We can summarize its operation in three key steps: (1) the simulation of a SN Ia light curve and (2) its fitting, grouped in Section I.2), and (3) a cosmology fit *via* the derivation of the SNe Ia distance (Section I.3).

## I.2 Simulation

In this section we present the key steps of the simulations with SNANA, as we perform them. In Section I.2.1 we introduce the fundamental concepts governing the operation of the software; the successive steps of generation (Section I.2.2), instrumental response (Section I.2.3) and detection (Section I.2.4) follow. A summary is proposed in Section I.2.5, with Figure I.3.

### I.2.1 Preparation of a simulation

Simulations with SNANA rely on two main libraries: (1) a host galaxy library (HOSTLIB) describing the relationship between a SN and its environment, and (2) a telescope instrumental characteristics library (SIMLIB) reproducing the observations of a survey and their survey conditions. In our approach to how our simulations work, these libraries precede the simulation process.

### I.2.1.1 HOSTLIB

Generally speaking, each galaxy in the HOSTLIB is described by :

- 1) An identification number (GALID);
- 2) A position of its center in the sky *via* the data of right ascension (RA\_GAL) and declination (DEC\_GAL);
- 3) A photometric redshift ( $z_{\text{TRUE}}$ );
- 4) Its magnitudes in the different photometric bands ( $grizY_{\text{obs}}$ );
- 5) A Sérsic profile (describing the evolution of its intensity with the distance  $R$  from its center);
- 6) A mass in logarithmic scale in solar masses (LOGMASS) and its error (LOGMASS\_ERR).

These features allow, when simulating a supernova, to place it at a position around the Galactic center according to the Sérsic profile in order to determine the local surface luminosity and to add Poissonian noise to the subsequent light curves (Kessler et al. 2019). In our most general case, HOSTLIB also exhibits the characteristics that a SN from this host galaxy must meet:

- 7) Its color  $C$ ;
- 8) Its stretch  $X1$ ;
- 9) Its age *via* the LSSFR;
- 10) The associated magnitude step SNMAGSHIFT (see Chapter ?? ).

The HOSTLIB thus appears, in our study framework, as the key element allowing to vary the underlying distributions of the SNe Ia parameters. We describe the realization of the HOSTLIB and the different implementations of HOSTLIB in Chapter ?; for the moment we only describe its construction through the use of color and stretch parameter distributions generating the said table. This step is represented in the upper gray frame of Figure I.3, and an extract of one of our HOSTLIB is given in Figure I.1.

### I.2.1.2 SIMLIB

The SIMLIB, for its part, presents for each field of observation:

- 1) its name (for example, 82N in Figure I.2);
- 2) its RA and DECL coordinates;
- 3) the number of NOBS observations;
- 4) its galactic extinction MWEBV;

NR_highz.HOSTLIB										
GALID	RA_GAL	DEC_GAL	ZTRUE	g_obs..	n_Ser ...	LOGMASS	C	X1	LSSFR	SNMAGSHIFT
1	34.4579	-4.70279	0.908506	26.5384 ...	0.5..	9.23965	-0.0781484	0.0750751	1	0.065
2	34.7423	-4.70316	1.03694	23.9878 ...	0.5..	9.15756	-0.069378	-0.195195	1	0.065
3	34.9884	-4.70419	1.03077	22.6348 ...	0.5..	8.65909	-0.00361094	0.105105	1	0.065
4	34.9154	-4.70552	0.610123	21.9055 ...	0.5..	9.08866	0.0222294	-0.635636	1	0.065
5	34.368	-4.70245	1.46711	23.9215 ...	0.5..	11.216	-0.127838	-0.905906	0	-0.065
6	34.3359	-4.70219	1.34426	24.4587 ...	0.5..	8.65494	0.0113197	-0.245245	1	0.065
7	34.7635	-4.70222	1.58874	24.9358 ...	0.5..	9.08221	-0.137191	0.955956	1	0.065
8	34.3765	-4.70185	0.906368	26.615 ...	0.5..	9.01341	-0.0388782	0.895896	1	0.065
9	34.9026	-4.70123	1.03192	24.8315 ...	0.5..	9.25265	-0.0701101	1.0961	1	0.065
10	34.4398	-4.68424	1.17349	25.2497 ...	0.5..	9.06415	-0.0182467	1.32633	1	0.065
11	34.5885	-4.68422	0.644088	24.8833 ...	0.5..	10.081	0.0613798	0.965966	1	0.065
12	35.0154	-4.68397	0.842422	24.7775 ...	0.5..	9.24084	-0.0298566	-0.185185	1	0.065
13	34.389	-4.68399	0.426567	24.0152 ...	0.5..	9.58916	-3.51175e-05	0.385385	1	0.065
14	34.3406	-4.7024	0.945276	23.2322 ...	0.5..	10.2814	-0.0190914	-1.64665	0	-0.065
15	34.8999	-4.70154	1.12769	25.6951 ...	0.5..	9.80687	0.0584339	0.635636	1	0.065
16	34.8316	-4.70159	0.663146	24.3533 ...	0.5..	9.06501	-0.0408711	0.335335	1	0.065
17	34.6215	-4.70126	0.638762	24.27 ...	0.5..	10.953	0.175788	-1.98699	0	-0.065
18	34.8462	-4.70093	0.792681	25.3282 ...	0.5..	9.68392	-0.0749062	0.995996	1	0.065
19	34.6188	-4.70097	0.7654	27.2168 ...	0.5..	9.08105	-0.0971941	0.0950951	1	0.065
20	34.7099	-4.70075	1.21963	24.7118 ...	0.5..	7.2025	-0.0441532	-1.03604	1	0.065
21	34.5344	-4.70072	0.687485	24.2925 ...	0.5..	11.0805	0.086881	-1.44645	0	-0.065
22	34.3747	-4.70025	0.955046	25.4781 ...	0.5..	11.1925	-0.0701521	-0.825826	0	-0.065
23	34.5307	-4.70003	1.01174	25.1255 ...	0.5..	9.76396	0.007948	-0.205205	1	0.065

**Figure I.1** - Extract of a HOSTLIB used in our study, modified for the example.

5) the size of a pixel PIXSIZE.

and for each observation :

- 1) the observation date expressed in modified Julian days MJD associated with an identifier  
IDEXPT;
- 2) the filter concerned by the observation (FLT);
- 3) the characteristics of the CCD camera (CCD GAIN and CCD NOISE) at the time of acquisition;
- 4) atmospheric noise *via* the SKYSIG parameter giving the noise per pixel, summed over the effective aperture derived by a *Point Spread Function* (PSF) fit by the PSF1, PSF2 and PSF2/1 data (see Section 2 of [Kessler et al. 2009b](#), for details);
- 5) the average zero point ZPTAVG and its error ZPTERR allowing to convert the observed magnitude  $m$  into flux  $F$  in CCD counts *via* the relation  $F = 10^{-0.4(m - ZPTAVG)}$ .

In addition to these data, other features such as non-observation periods or flux corrections to be added to follow the telescope calibration are shown. Figure I.2 shows an extract from the SIMLIB of the SDSS telescope.

In addition to these libraries, each survey has an associated weight map (WEIGHTMAP), which will be used to weight the HOSTLIB on the mass parameter so that the galaxies to which the SNe Ia are connected correspond to the mass distribution of host galaxies actually observed by the survey. An example is shown under

SDSS.SIMLIB

SURVEY: SDSS

GENSKIP\_PEAKMJD: 53705 53975

GENSKIP\_PEAKMJD: 54060 54345

BEGIN

FILTERS: ugriz

53705 53975

54060 54345

LIBGENSunMar 11 15:44:23 CDT 2012

TELESCOPE: SDSS

# skip the off-season #

ditto

# =====

LIBID: 1

RA: 26.430172

FIELD: 82N

(from 2005 libid 1)

DECL: 0.844033

MWEBV: 0.026

PIXSIZE: 0.400

#

#

MJD

IDEXPT

FLT

GAIN

NOISE

SKYSIG (pixels)

RATIO

ZPTAVG

ZPTERR

S: 53616.383

556600405

u

1.47

4.48

4.83

1.89

3.69

0.225

27.58

0.017

S: 53616.383

556600405

g

4.05

4.25

4.04

1.85

3.61

0.247

28.39

0.008

S: 53616.383

556600405

r

4.72

4.25

5.28

1.64

3.62

0.142

28.22

0.010

S: 53616.383

556600405

i

4.64

12.99

6.95

1.60

3.81

0.103

27.88

0.009

S: 53616.383

556600405

z

3.48

4.70

6.91

1.74

3.75

0.131

26.54

0.011

S: 53626.359

560300625

u

1.47

4.48

4.60

1.71

3.62

0.116

27.47

0.017

S: 53626.359

560300625

g

4.05

4.25

4.40

1.83

3.50

0.282

28.03

0.008

S: 53626.359

560300625

r

4.72

4.25

5.87

1.64

3.65

0.112

27.99

0.010

S: 53626.359

560300625

i

4.64

12.99

6.54

1.47

3.56

0.070

27.86

0.009

S: 53626.359

560300625

z

3.48

4.70

6.73

1.64

3.88

0.110

24.46

0.011

S: 53628.344

561000626

u

1.47

4.48

11.16

1.56

3.38

0.070

26.97

0.017

S: 53628.344

561000626

g

4.05

4.25

11.61

1.59

3.28

0.095

28.36

0.008

S: 53628.344

561000626

r

4.72

4.25

9.24

1.40

3.36

0.059

28.19

0.010

S: 53628.344

561000626

i

4.64

12.99

9.27

1.33

3.46

0.049

27.89

0.009

S: 53628.344

561000626

z

3.48

4.70

7.95

1.39

3.54

0.046

26.14

0.011

etc...

**Figure I.2** - Extract from the SDSS SIMLIB. Data from [Kessler et al. \(2013\)](#).

the boxed title WEIGHTMAP in Figure I.3. This library is of key importance since the inclusion of host mass as an environmental tracer of the underlying properties of SNe Ia (see Chapter ?? ); when a HOSTLIB does not include a magnitude walk, that is which adds to galaxies of  $M_* < 1 \times 10^{10} M_\odot$  a magnitude variation of 0.025 mag and to those of  $M_* > 1 \times 10^{10} M_\odot$  a variation of -0.025 mag to match mass-based magnitude walk observations.

The simulation of a supernova then follows 3 major steps, described in [Kessler et al \(2019\)](#):

- 1) Generation of the source and application of cosmological effects, simulating the propagation of its light from its origin to the top of the atmosphere;
- 2) Simulation of the instrumental response according to the survey (e.g. conversion of the magnitude into photon flux captured by a CCD camera, instrument noise. . . ) ;
- 3) Simulation of the detection, including the criteria for the SN to be a candidate for observation (see Chapter ?? ) and the spectroscopic efficiency of the survey.

## I.2.2 Model generation

We use the SALT2 spectral model from [Guy et al. \(2007\)](#) and previously described Chapter ?? to generate a SN Ia. It is initialized in a resting reference frame for epochs between 20 days before and  $\approx 70$  days after the emission maximum. At each

SN is thus associated a redshift ( $z_{\text{CMB}}$  in the cosmic microwave background reference frame) from a SNe Ia rate model (different depending on the survey), an emission maximum  $t_0$  randomly chosen on a range before and after the survey observation period, and a value of stretch  $x_1$  and color  $c$ . Our approach is to draw these parameters from the HOSTLIB, weighted by the WEIGHTMAP of the survey, by matching the initially chosen redshift with one of the table entries. This draw also gives the value of the magnitude step to apply. This is how the model generation is made dependent on its environment. This step is illustrated by the "Drawing" part (in pink) of Figure I.3, considered as the input step in a simulation and numbered "1", leading to the HOSTLIB parameters illustrated in the "HOSTLIB Creation" part (numbered "2") by a pink dotted arrow labeled "Link with the environment". The assignment of these two parameters varies according to the correlation postulates we have implemented, we will return to this in the next chapter.

With the chosen redshift, at this step is defined a real distance,  $\mu_{\text{vrai}}$ , via its definition (given Chapter ?? ), assuming an underlying cosmology. In our case, we use the  $w\Lambda\text{CDM}$  model with values defined in Table I.1.

**Table I.1** - Value of the cosmological parameters used for the determination of the real distance modulus of the simulated SN.

$H_0$	$\Omega_M$	$\Omega_\Lambda$	$w_0$
70.0 km Mpc-1 s-		0,3150,	-1,00
1	685		

Using the other chosen parameters, we also have:

$$\mu_{\text{true}} = mb_{\text{true}} - M + \alpha_{\text{ref}} x_{1,\text{true}} - \beta_{\text{ref}} c_{\text{true}} + \gamma_{\text{env}} \quad (\text{I.1})$$

where  $\alpha_{\text{ref}}$  and  $\beta_{\text{ref}}$  are the coefficients of the linear magnitude-stretch and magnitude-color correlations, respectively (see Chapter ?? ). In this equation, their values are fixed at 0.145 and 3.1, respectively, following the analysis of Popovic et al. (2021).  $M$  is also fixed, at -19.3 mag. The magnitude step  $\gamma_{\text{env}}$  varies depending on the source of the correlation to the environment: for a correlation with the mass  $M_*$  of the host galaxy,  $\gamma_{\text{env}} = 0.025 \text{ mag}$  for  $M_* > 10^{10} M_\odot$  and  $M_* < 10^{10} M_\odot$  respectively; for a correlation with the age of the SN,  $\gamma_{\text{env}} = 0.065 \text{ mag}$  for both young and old SNe Ia, respectively. In this way, we can deduce the value of  $mb_{\text{vrai}}$  from the apparent magnitude.

The model then has intrinsic dispersion effects (in our case the one described in Guy et al. (2010), named G10 ), weak lensing, redshift to place it in the heliocentric frame of reference, and Milky Way galactic extinction, applied to  $mb_{\text{vrai}}$ . These different effects lead to simulate a magnitude at the top of the atmosphere, before an instrument acquires it. The details of these procedures are developed in Kessler et al. (2019). This section is illustrated by the blue dotted arrow labeled "Generation" going from the "HOSTLIB Creation" section numbered "2" to the representation of a theoretical time series of a SN at the beginning of the section "Instrument" in blue, numbered "3".



### I.2.3 Instrumental response

Once the time series of the SN spectrum is formed, the program simulates the actual received flux and noise measured by the reproduced sounding telescope. As described in Section I.2.1, this is set by the observation logs of the soundings summarized in SIMLIB. It allows to apply the observing qualities of the telescope to each epoch of the time series, mimicking the acquisition or not of photometric points by the optical bands of the instrument and leading to the establishment of a light curve. This step is represented in the "Instrument" part in blue in Figure I.3, numbered "3". It is also in this part, but not represented on the figure, that a Poissonian noise is added to the measurement according to the local surface luminosity induced by the position of the SN with respect to the center of its host galaxy. These steps simulate the transformation of the signal at the top of the atmosphere to the signal actually received on Earth.

According to the package author in Kessler et al. (2019), SNANA simulations are ideally suited for sliding search surveys for which the same instrument is used to detect and measure light curves, e.g., the PS1, SDSS, and SNLS surveys we presented Chapter ??; in contrast, the LOWZ sample (see Section ?? which is both a targeted search and relies on follow-ups from independent research programs, does not have research data logs that allow for ideal simulation, and thus requires additional approximations and assumptions. For more detail on these two paragraphs, see Section 6 of Kessler et al. (2019).

### I.2.4 Selection and adjustment

As described in Chapter ? , each of the SNe Ia surveys observing the sky acquires successive images in search of transient events, but only triggers the continuous acquisition and tracking of a candidate if its light curve meets certain criteria. This step is included in the SNANA simulations process, and includes the signal-to-noise ratio of the data (SNR) and the number of detections relative to the emission peak ( $T_{\text{rest}}$ ) that each survey requires in its search. Finally, the spectroscopic efficiency as a function of magnitude is simulated ahead of the simulation, *via* the use of fake SN data, and is used to perform data selection.

The fitting part of the detected data is also done with SALT2 and is therefore not detailed again here, but a whole SNANA course is devoted to it. Briefly, this fitting extracts the parameters  $m_B$ ,  $x_1$ ,  $c$  and  $t_0$  from the light curves passing the detection criteria.  $m_B$  corresponds to the magnitude of the SN,  $x_1$  to its stretch,  $c$  to its color and  $t_0$  to the maximum brightness time. From their values, an additional cut is made to keep only the cosmological quality data, in particular having to check  $3 < x_1 < 3$ ; the other SNe Ia will not pass the selection on the fit and will remain at the detection stage.

This step is imaged in the green "Selection" box numbered "4" in Figure I.3, where we differentiated SNe that possess cosmological qualities from those only detected but rejected in the next step by orange and green frames, respectively, accompanied by the labels "Fit retained" and "Detection rejected", respectively.

### I.2.5 Summary

Starting from HOSTLIB, SIMLIB, WEIGHTMAP and spectroscopic efficiency tables, we describe the steps of a simulation in the following order corresponding to the box numbers in Figure I.3 :

- 1) Selection of a redshift from a SNe Ia rate model;
- 2) Matching with a HOSTLIB host galaxy and generating the model with corresponding stretch and color parameters;
- 3) Simulation of the instrumental response leading to the light curve;
- 4) Application of data detection and selection criteria;
- 5) Retention of data passing the previous steps.

In the figure, the redshift distribution is from Equation 6 of Perrett et al. (2012) with values from Popovic et al. (2021) based on the study of Scolnic et al. (2018) :

$$\text{SNR}_{\text{Ia}}(z) = r_0 (1+z)^\alpha \quad \text{with} \quad \begin{array}{l} r_0 = 2.6 \times 10^{-5} \text{ SNe an}^{-1} \text{ Mpc}^{-3} \\ \alpha = 2 \quad \text{.2 for SDSS, PS1, SNLS} \\ \quad \quad \quad 1.5 \text{ for LOWZ} \end{array} \quad (\text{I.2})$$

In Boxes 1, 3, 4, the graphs use values and data from SDSS (Sako et al. 2018). WEIGHTMAP and spectroscopic efficiency are from Popovic et al. (2021).

## I.3 Bias correction and cosmology

In this section we present the cosmology adjuster step with SNANA bias corrections based on the *BEAMS with Bias Correction* method (BBC, Kessler and Scolnic 2017). BEAMS stands for *Bayesian Estimation Applied to Multiple Species*, an adjuster method established in Kunz et al. (2007) to realistically account for non-Ia data contamination in SNe Ia data that affects the study of cosmology with SNe Ia. In our case, we do not simulate non-Ia SNe and ignore the related likelihood terms.

### I.3.1 Presentation

As introduced in Section I.2.2, without measurement bias the distance modulus of the simulated SN would be  $\mu_{\text{vrai}}$  from Equation I.1, and a fit of the Hubble diagram with these values would yield only the input cosmology. With the values of  $m_B$ ,  $x_1$ ,  $c$  and the characteristics of the environment of the SALT2.4 fit that will have passed the previous steps, one would have a distance modulus of the form

$$\mu = m_B - M + \alpha x_1 - \beta c + \gamma_{\text{env}} \quad (\text{I.3})$$



The figure consists of two vertically stacked plots. The top plot is titled "WEIGHTMAP" and shows the probability  $P(M)$  on the y-axis (ranging from 0 to 1) versus redshift  $z$  on the x-axis (ranging from 0 to 1). The curve is a jagged line representing a probability distribution, with a primary peak around  $z=0.5$  reaching a value of approximately 1.0. The bottom plot is titled "Mhost" and shows the number of galaxies  $N(1-15)$  and number of galaxies  $N(1-15)$  on the y-axis (ranging from 0 to 10) versus redshift  $z$  on the x-axis (ranging from 0 to 1). The curve is a smooth, solid line representing a distribution, with a peak around  $z=0.5$  reaching a value of approximately 10. Both plots have a light blue background and a white grid.

Figure 1 displays the spectral analysis of the 10000 Å region. The top panel shows the observed spectrum (black) and model components (colored lines) for the 10000 Å region. The bottom panel shows the residuals (black) and model components (colored lines) for the 10000 Å region. The right panel shows the residuals (black) and model components (colored lines) for the 10000 Å region.

## SELECTION

**Detection**

**Quality cuts**

$r_{\text{test}} < 0$	$r_{\text{test}} > 10$	$\text{SNR} > 5$	$gri - z < 1$	$x1 < 3 \dots$	
✓					...
✓	✓		✓		...
			✓		...
✓	✓		✓	✓	...

Detection rejected

Retention and adjustment

A fit of the Hubble diagram could give an offset to this model, but remains suboptimal since the selection and fitting biases of light curves are not taken into account. The interest of BBC is to include the measurement of these biases in the calculation of the distance modulus; thus the SN is assigned a distance modulus according to the framework of the BBC method, defined in (Popovic et al. 2021) :

$$\mu^* = m_B + \alpha x_1 - \beta c - M_{Z_i} + \delta\mu_{\text{env}} + \delta\mu_{\text{bias}}$$

(I.4) where the star indicates a bias-corrected magnitude.

$\delta\mu_{\text{env}}$  is the bias on the luminosity depending on the SN environment, in our case a mass-based ("mass step") or age-based ("age step") magnitude step, of the form

$$\delta\mu_{\text{env}} = \gamma_{\text{env}} \times \left( 1 + e^{(X_* - S)/\tau_X} \right)^{-1/2} \quad (\text{I.5})$$

with  $X_* = \log(M_*)$ ;  $S = 10.0$  the value of the massive or nonmassive host separation;  $\tau_X$  the width of the magnitude step; and  $\gamma_{\text{env}}$  the magnitude of the magnitude difference between SNe Ia with massive ( $X_* > S$ ) or nonmassive ( $X_* < S$ ) hosts for the *mass step* or between old or young SNe Ia for the *age step*. Because the software does not yet allow the use of age as a tracer, this implementation of the bias due to the age of the environment is not representative of reality; we discuss this in the next chapter.  $S$  and  $\tau_X$  are fixed values.

$\delta\mu_{\text{bias}}$  is the correction to the distance modulus. This is measured using a large sample size,  $N \sim 10^6$  simulated SNe Ia, called BiasCor. There are different ways to measure this bias depending on the variables with which it is calculated, which we present in the following sections.

The parameters  $M_{Z_i}$  are defined in the framework of the SALT2mu fit, defined in Marriner et al. (2011) and used in the BBC framework. This program allows  $\alpha$  and  $\beta$  to be fitted without joint adjustment of the cosmological parameters: these are first fixed, and then the program defines redshift intervals small enough to consider that within them the SNe Ia are cosmologically independent. The  $M_{Z_i}$  are then the distance deviations in these redshift intervals  $z_i$ , such that  $\mu = \mu_{\text{vrai}}$  when the initial values of  $m_B$ ,  $x_1$  and  $c$  from the Generation part (Section I.2.2) are entered instead of the fitted values in Equation I.4. These are the values that are used to fit the cosmology. Indeed, for the fit we start from a flat cosmological model  $w\text{CDM}$  where  $\Omega_M + \Omega_\Lambda = 1$ , to define (Kessler and Scolnic 2017):

$$\mu_{\text{modèle}} = -2.5 \log \left( \frac{d_L}{10 \text{ pc}} \right) \quad \text{avec} \quad (\text{I.6})$$

$$d_L(z, w, \Omega_M) = (1+z) \frac{c}{H_0} \quad \text{and} \quad (\text{I.7})$$

$$E(z) = \frac{\Omega_M}{\Omega_M + \Omega_\Lambda} (1+z)^3 + \frac{E(z)}{\Omega_\Lambda} (1+z)^{3(1+w)} \quad (\text{I.8})$$

and SALT2mu uses the MINUIT package<sup>1</sup> (James and Roos 1975) to adjust the quantity:

$$\chi^2_{\text{HD}} = \sum_i \frac{(\mu_i - \mu_{\text{modèle}} - M_{Z_i})^2}{\sigma_i^2} \quad (\text{I.9})$$

1. [www.cern.ch/minuit](http://www.cern.ch/minuit)

with  $\sigma_{\mu,i}$  the uncertainties (including those on the SALT2-fitted values and their covariances, those due to weak lensing, redshift uncertainty, and intrinsic dispersion). Rather than adjusting  $\mu_{model}$  for cosmological parameters, we keep them at reference values (see Table I.1) and it is the  $M_{z,i}$  that are adjusted. This allows the underlying cosmology to vary without repeating the adjustment of  $\alpha$  and  $\beta$ . Thus, with this formalism,  $\alpha, \beta, \gamma_{env}, M_{z,i}$  and  $\sigma_{\mu}$  are the fitted parameters.

The cosmological parameters are finally obtained from these parameters fitted by the wfit program, yielding  $w$  and  $\Omega_M$ . We use a Gaussian prior distribution for  $\Omega_M$  with a mean at 0.315 and a width of 0.005, and flat for  $w$  with bounds  $-1.5 < w < 0.5$ . For more details on how it works, see Section 5.6 of Kessler and Scolnic (2017).

We now discuss the different implementations of BBC for the calculation of  $\delta\mu_{bias}$ .

### I.3.2 BBC1D

Originally, it is computed along a single dimension, the redshift, and affects only the peak emission magnitude  $m_B$ . We call this implementation BBC1D. It is based on redshift intervals of typical size  $< 0.1$  carving out the BiasCor sample. In each of these intervals, we compute the weighted average of the events belonging to it, and it is defined at a position  $z_i$  also derived from the weighted average of the redshifts in the interval. The value of the bias  $\delta\mu_{bias} = \delta m_B$  to be added to the measured distance modulus is then determined by a linear interpolation of the previous values, and we obtain the corrected distance modulus :

$$\begin{aligned}\mu^* &= m_B^* + \alpha x_1 - \beta c - M_{z,i} + \delta\mu_{env} \\ &= (m_B - \delta m_B) + \alpha x_1 - \beta c - M_{z,i} + \delta\mu_{env} \\ &= m_B + \alpha x_1 - \beta c - M_{z,i} + \delta\mu_{env} + \delta\mu_{bias}(z)\end{aligned}\tag{I.10}$$

with  $m_B^*$  the magnitude corrected according to its  $z$  position: all SNe belonging to the same redshift interval are corrected by the same  $\delta m_B$ .

These corrected distance moduli are then processed by SALT2mu, which returns the adjusted values  $\alpha, \beta, \gamma_{env}, M_{z,i}$ , and  $\sigma_{\mu}$ . After this step, the wfit software adjusts the values of  $M_{z,i}$  as a function of redshift to have the cosmological parameters. A schematic of the operation is given in Figure I.4.

### I.3.3 BBC5D

Developed in Kessler and Scolnic (2017), this method is an extension of BBC1D, this time correcting for  $m_B, x_1$  and  $c$  using the BiasCor sample. Rather than sequencing it solely in redshift to determine  $\delta m_B$ , it is divided into cells of sizes (0.05; 0.50; 0.05) respectively. The corrections  $\delta m_B, \delta x_1$  and  $\delta c$  to be applied are then calculated from the interpolation of the weighted averages of the SNe in each cell. We represent this process Figure I.5, where the superscripts correspond to the intervals according to  $c, x_1$  and  $z$  respectively, for which the total number of intervals is  $C, X$  and  $Z$ , respectively; the subscript  $p$  indicates the parameter to be selected in the cell in question to obtain the corresponding bias.

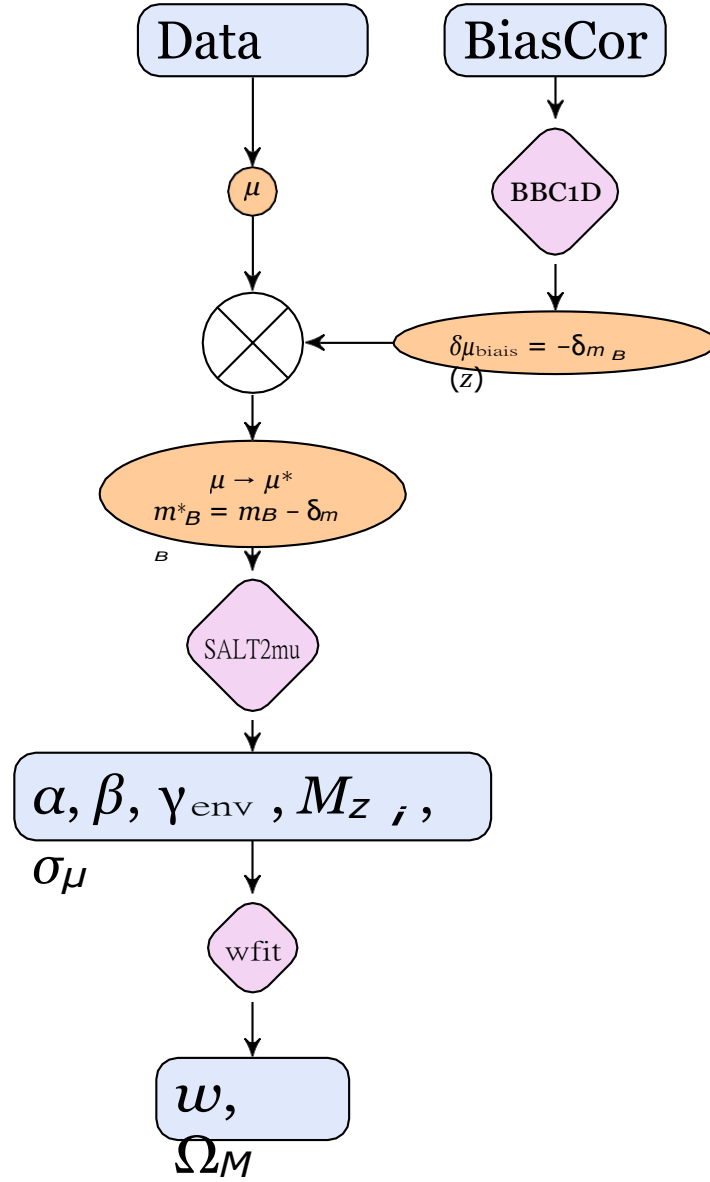


**Figure I.4** - Schematic of the BBC bias correction method when in its 1-dimensional version. From the BiasCor sample are determined the values  $\delta\mu_{\text{bias}}$  to be added to the distance modulus by slicing it into redshift intervals to calculate the weighted average there. With the data they allow to determine the corrected distance moduli  $\mu^*$ , which are then processed by SALT2mu to have the  $\alpha, \beta, \gamma_{\text{env}}, M_{Z,i}$  and  $\sigma_\mu$  that allow the cosmological fit by wfit.

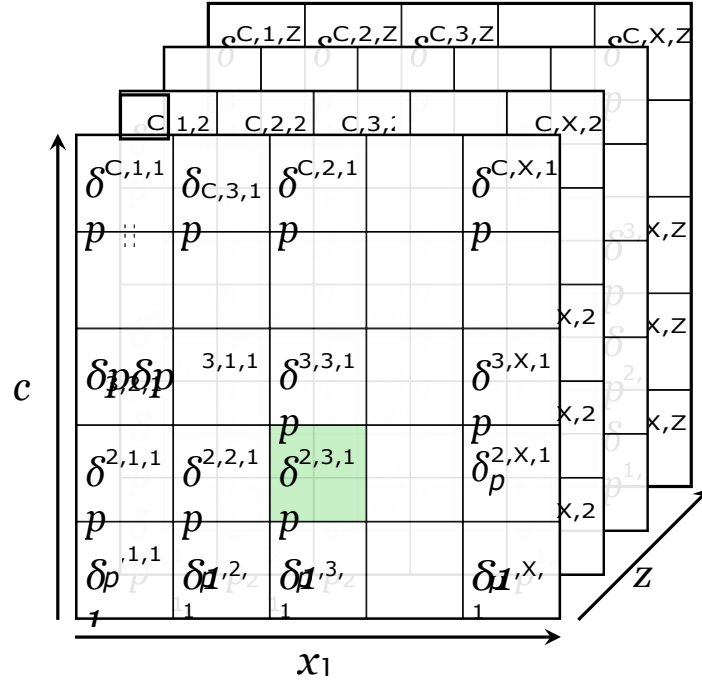


**Figure I.5** – Schéma de fonctionnement du découpage de l'échantillon BiasCor en 3 dimensions  $x_1$ ,  $c$ ,  $z$  de la méthode BBC5D. Pour une supernova dont les valeurs de  $c$ ,  $x_1$ ,  $z$  sont dans les intervalles 2, 3, 1, respectivement, les valeurs  $\delta_{m_B}$ ,  $\delta_{x_1}$  et  $\delta_c$  seront celles issues de la cellule coloriée en vert.

With this division, we obtain this time :

$$\begin{aligned}
 \mu^* &= m_B^* + \alpha x_1^* - \beta c^* - M_{z_i} + \delta\mu_{\text{env}} \\
 &= (m_B - \delta_{m_B}) + \alpha(x_1 - \delta_{x_1}) - \beta(c - \delta_c) - M_{z_i} + \delta\mu_{\text{env}} \\
 &= m_B + \alpha x_1 - \beta c - M_{z_i} + \delta\mu_{\text{env}} + \delta\mu_{\text{biais}}(z, x_1, c, \alpha, \beta)
 \end{aligned} \tag{I.11}$$

with

$$\delta\mu_{\text{biais}} = (\delta_{m_B} + \alpha\delta_{x_1} - \beta\delta_c) \tag{I.12}$$

C'est de la dimension de  $\delta\mu_{\text{biais}}$  que BBC5D tire son nom. En effet, une version 3D avec uniquement le découpage susmentionné peut exister (Scolnic et Kessler 2016), mais il se trouve que les valeurs de corrections de biais dépendent des valeurs de  $\alpha$  et  $\beta$  utilisées. Pour reproduire cette corrélation et étant donné que ces coefficients ont des valeurs discrètes, ces paramètres sont générés sur une grille de taille  $2 \times 2$ , encapsulant les valeurs trouvées par les études précédentes, et pour chacune de ces valeurs sont définies les matrices découpées en 3D précédentes. Nous utilisons  $\alpha = [0,10 ; 0,20]$  et  $\beta = [2,8 ; 3,4]$  (étant donné que notre dispersion intrinsèque est basée sur G10). Nous illustrons ce principe Figure I.6.

The final correction values are the 3-dimensional interpolations of  $\delta\mu_{\text{biais}}$  at each value of  $\alpha$  and  $\beta$  for each iteration of the BBC fit, whose results are also linearly interpolated. Once these values are corrected,  $\alpha$ ,  $\beta$ ,  $\gamma_{\text{env}}$ ,  $M_{z_i}$ , and  $\sigma_\mu$  are minimized by SALT2mu, and the redshift fit of  $M_{z_i}$  by wfit yields the cosmological parameter values. This operation is summarized in Figure I.7.

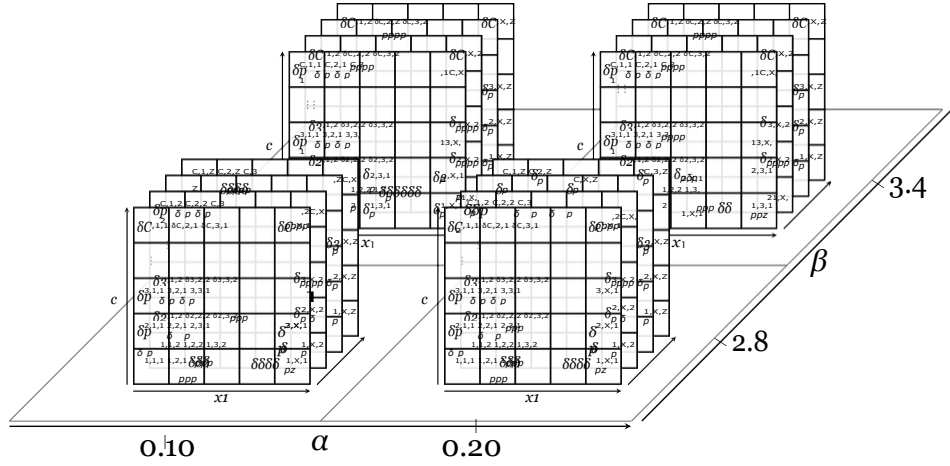


**Figure I.6** - Schematic of how the 5D bias correction of the BBC5D method works: the parameters  $\alpha$  and  $\beta$  are generated on a grid of size 2 2, and to each of the values of this grid are associated the BiasCor sample cut matrices in 3 dimensions:  $x_1$ ,  $c$  and  $z$ . The final values to be added to the distance modulus of the simulated SN results from the 5D interpolation of the best fit.

### I.3.4 BBC7D

In the work of [Smith et al. \(2020\)](#), it was determined that the  $\gamma_{\text{env}}$  parameter fitted by BBC5D had a bias if the sample being analyzed had correlations between the stretch and/or color parameters with the mass of the host galaxy. To account for these biases in the *mass step*, [Popovic et al. \(2021\)](#) then introduced two new dimensions to the  $\delta\mu_{\text{bias}}$  term in Equation I.11:  $\theta$ , a generic magnitude shift, and  $M_*$  the mass of the host galaxy.

The idea of this addition is to assign a magnitude shift of  $+\theta$  to one *random* half of the BiasCor sample, and  $\theta$  to the other half; this parameter, which is completely uncorrelated with environmental properties, is therefore inherently different from  $\gamma_{\text{env}}$ , and allows greater flexibility than using  $\delta\mu_{\text{env}} = \gamma_{\text{env}}/2$  for  $X_* \gtrless S$ , respectively.

These parameters are used at each step of the BBC fit, going from a  $\delta\mu_{\text{bias}}$  in 5 dimensions ( $\mathbf{x} = \{z, x_1, c, \alpha, \beta\}$ ) to 7 dimensions  $\{\rightarrow -\mathbf{x}_5, \theta, M_*\}$ .  $\delta\mu_{\text{bias}}$  is interpolated to the first six, and evaluated in intervals according to  $M_*$ . The  $\delta\mu_{\text{env}}$  values allow the BiasCor sample to be interpolated between  $\pm\theta$  following :

$$\delta\mu_{\text{bias}} = f \times \delta\mu_{\text{bias}}(\mathbf{x}, +\theta, M_*) + (1 - f) \times \delta\mu_{\text{bias}}(\mathbf{x}, -\theta, M_*) \quad (\text{I.13})$$

with  $f = \frac{\delta\mu_{\text{env}} + \theta}{2\theta}$ . Since  $\theta$  is independent of the SNe parameters, it allows us to examine correlations betw any host galaxy property and the magnitude of SNe Ia.

It is with this BBC formalism that we treat our simulations in the next chapter.

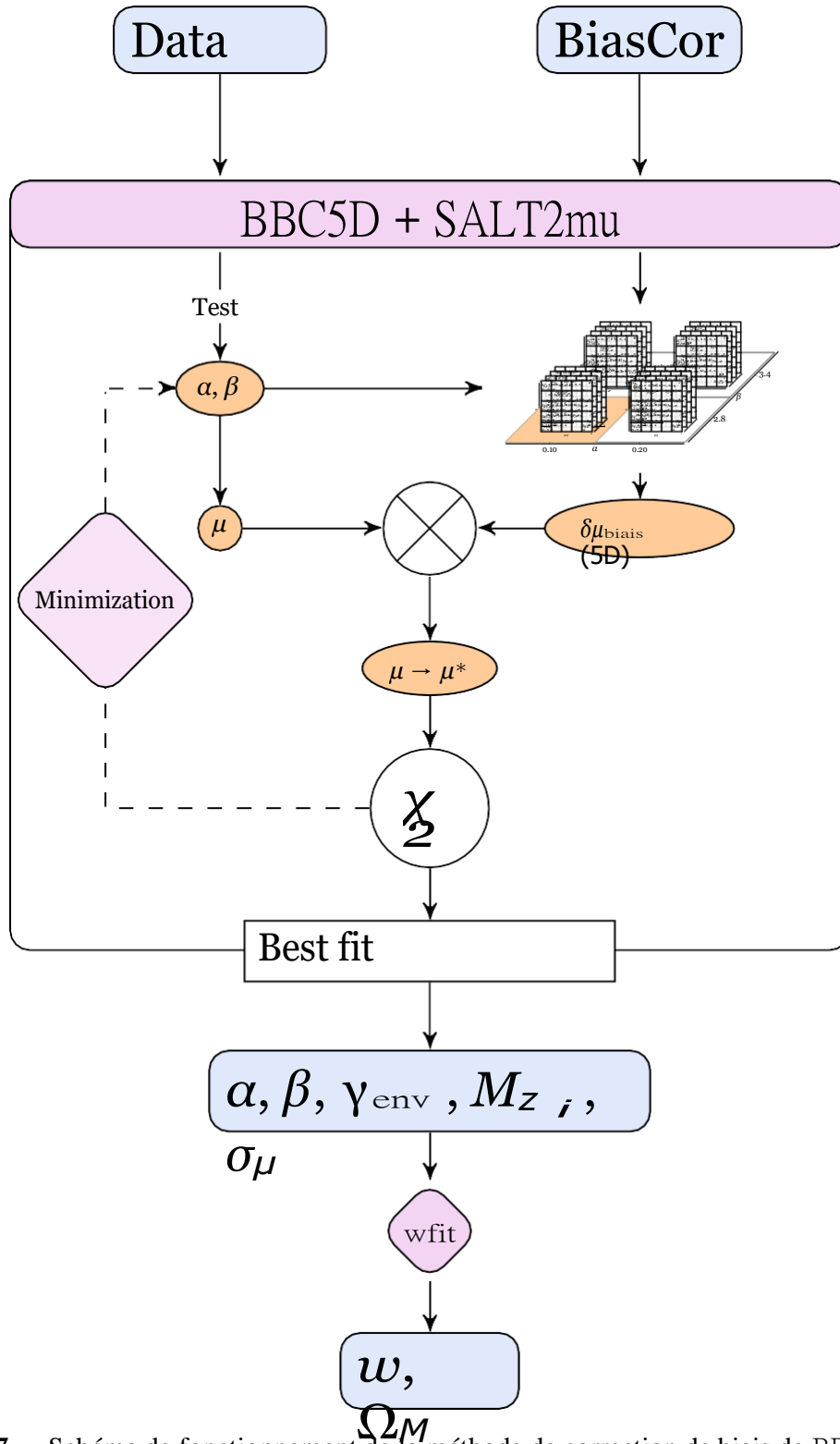


**Figure I.7** – Schéma de fonctionnement de la méthode de correction de biais de BBC lorsqu'elle est dans sa version à 5 dimensions. Contrairement à BBC1D, ici l'ajustement de  $\alpha$  et  $\beta$  se fait en même temps que la correction de biais, cette dernière étant dépendante des valeurs des premières. Les valeurs de  $\delta\mu_{\text{biais}}$  à ajouter à  $\mu$  et de  $\alpha$  et  $\beta$  sont les interpolations du meilleur ajustement, donnant en sortie des  $M_{z_i}$  qui permettent l'ajustement par wfit.



## Figures

---

I.1 Extract from a HOSTLIB used in our study ... ..	4
I.2 Extract from the SDSS SIMLIB .....	5
I.3 Schematic diagram of a simulation with SNANA ... ..	9
I.4 Schematic of the BBC1D12 bias correction method	
I.5 Schematic diagram of the BiasCor sample slicing in 3 dimensions $x_1$ , $c$ , $z$ of the BBC5D method13	
I.6 Schematic diagram of the 5-dimensional bias correction of the BBC5D14 method	
I.7 Schematic of the BBC5D15 bias correction method	

---

## Tables

---

I.1 Value of the cosmological parameters used for the determination of the real distance modulus of the simulated SN ... ..	6
---	---

---

# Bibliography

Betoule M. , Kessler R. , Guy J. et al. 2014, "Improved cosmological constraints from a joint analysis of the SDSS-II and SNLS supernova samples," [A&A](#), [568](#), [A22](#)

[↑ Section I](#)

Conley A. , Guy J. , Sullivan M. et al. 2011, "Supernova Constraints and Systematic Uncertainties from the First Three Years of the Supernova Legacy Survey," [ApJS](#), [192](#), [1](#) [↑ Section I](#)

Guy J. , Astier P. , Baumont S. et al. 2007, "SALT2: using distant supernovae to improve the use of type Ia supernovae as distance indicators", [A&A](#), [466](#), [11](#) [↑ Section I.2.2](#)

Guy J. , Sullivan M. , Conley A. et al. 2010, "The Supernova Legacy Survey 3-year sample: Type Ia supernovae photometric distances and cosmological constraints," [A&A](#), [523](#), [A7](#) [↑ Section I.2.2](#), [↑ Section I.3.3](#)

James F. and Roos M. 1975, "Minuit - a system for function minimization and analysis of the parameter errors and correlations," [Computer Physics Communications](#), [10](#), [343](#)

[↑ Section I.3.1](#)

Kessler R. , Becker A. C. , Cinabro D. et al. 2009a, "First-Year Sloan Digital Sky Survey-II Supernova Results: Hubble Diagram and Cosmological Parameters," [ApJS](#), [185](#), [32](#) [↑ Section I](#)

Kessler R. , Bernstein J. P. , Cinabro D. et al. 2009b, "SNANA: A Public Software Package for Supernova Analysis," [PASP](#), [121](#), [1028](#) [↑ Section I](#), [↑ Section I.1](#), [↑ Section 4\)](#)

Kessler R. , Brout D. , D'Andrea C. B. et al. 2019, 'First cosmology results using Type Ia supernova from the Dark Energy Survey: simulations to correct supernova distance biases', [MNRAS](#), [485](#), [1171](#) [↑ Section I.1](#), [↑ Section I.2.1.1](#), [↑ Section I.2.1.2](#), [↑ Section I.2.2](#), [↑ Section I.2.3](#)

Kessler R. , Guy J. , Marriner J. et al. 2013, "Testing Models of Intrinsic Brightness Variations in Type Ia Supernovae and Their Impact on Measuring Cosmological Parameters," [ApJ](#), [764](#), [48](#) [↑ Section I.2](#)

Kessler R. and Scolnic D. 2017, "Correcting Type Ia Supernova Distances for Selection Biases and Contamination in Photometrically Identified Samples," [ApJ](#), [836](#), [56](#) [↑ Section I.3](#), [↑ Section I.3.1](#), [↑ Section I.3.1](#), [↑ Section I.3.3](#)

Kunz M. , Bassett B. A. and Hlozek R. A. 2007, "Bayesian estimation applied to multiple species," [Phys. Rev. D](#), [75](#), [103508](#) [↑ Section I.3](#)



- Marriner J. , Bernstein J. P. , Kessler R. et al. 2011, "A More General Model for the Intrinsic Scatter in Type Ia Supernova Distance Moduli," [ApJ](#), 740, 72 [Section I.3.1](#)
- Perrett K. , Sullivan M. , Conley A. et al. 2012, "Evolution in the Volumetric Type Ia Supernova Rate from the Supernova Legacy Survey," [AJ](#), 144, 59 [Section I.2.5](#)
- Popovic B. , Brout D. , Kessler R. , Scolnic D. , and Lu L. 2021, "Improved Treatment of Host-galaxy Correlations in Cosmological Analyses with Type Ia Supernovae," [ApJ](#), 913, 49 [Section I.2.2](#), [Section I.2.5](#), [Section I.3.1](#), [Section I.3.4](#)
- Sako M. , Bassett B. , Becker A. C. et al. 2018, "The Data Release of the Sloan Digital Sky Survey-II Supernova Survey," [PASP](#), 130, 064002 [Section I.2.5](#)
- Scolnic D. and Kessler R. 2016, "Measuring Type Ia Supernova Populations of Stretch and Color and Predicting Distance Biases," [ApJ](#), 822, L35 [Section I.3.3](#)
- Scolnic D. M. , Jones D. O. , Rest A. et al. 2018, "The Complete Light-curve Sample of Spectroscopically Confirmed SNe Ia from Pan-STARRS1 and Cosmological Constraints from the Combined Pantheon Sample," [ApJ](#), 859, 101 [Section I.2.5](#)
- Smith M. , Sullivan M. , Wiseman P. et al. 2020, "First cosmology results using type Ia supernovae from the Dark Energy Survey: the effect of host galaxy properties on supernova luminosity," [MNRAS](#), 494, 4426 [Section I](#), [Section I.3.4](#)